International Journal of Earth, Energy and Environmental Sciences
ISSN: 2517-942X
Vol:9, No:6, 2015

Effects of Hydrogen-Ion Irritation on the Microstructure and Hardness of Fe-0.2wt.%V Alloy

Jing Zhang, Yongqin Chang, Yongwei Wang, Xiaolin Li, Shaoning Jiang, Farong Wan, Yi Long

***Abstract*—**Microstructural and hardening changes of Fe-0.2wt.%V alloy and pure Fe irradiated with 100 keV hydrogen ions at room temperature were investigated. It was found that dislocation density varies dramatically after irradiation, ranging from dislocation free to dense areas with tangled and complex dislocation configuration. As the irradiated Fe-0.2wt.%V samples were annealed at 773 K, the irradiation-induced dislocation loops disappear, while many small precipitates with enriched C distribute in the matrix. Some large precipitates with enriched V were also observed. The hardness of Fe-0.2wt.%V alloy and pure Fe increases after irradiation, which ascribes to the formation of dislocation loops in the irradiated specimens. Compared with pure Fe, the size of the irradiation-introduced dislocation loops in Fe-0.2wt.%V alloy decreases and the density increases, the change of the hardness also decreases.

***Keywords*—**Irradiation, Fe-0.2wt.%V alloy, microstructures, hardness.

I. Introduction

REDUCED activation ferritic/martensitic (RAFM) steel is a promising material for the first wall of future fusion reactor that will suffer irradiation damage from 14 MeV fusion neutrons [1], [2]. At the same time, neutron irradiation will also produce transmutation reactions of (n,p) and (n,a) and result in the formation of helium and hydrogen in materials, such kinds of gas atoms may promote damage behavior during irradiation. Ion irradiation is always chosen to simulate the damage induced by fast neutrons for several reasons including avoidance of activated material due to neutron irradiation and reduction of irradiation times. Interaction between helium and irradiation-introduced defects has been extensively investigated [3]-[5]. Although H production rate in the reactor is high and most of H is believed to diffuse out of materials, it also introduces some defects in the materials. C. Liu et al. investigated the embrittlement introduced by hydrogen in UROFER97, and found that H content decreases after testing at higher temperature, while some specimens still contain significant amounts of hydrogen even after testing at 350℃ [6]. T. Hino et al. reported that amounts of retained deuterium increases as the damage caused by hydrogen-ion irradiation in F82H increases [7]. Y. Huang et al. investigated the nature of the dislocation loops induced by H-ion irradiation at room temperature in pure iron [8]. When RAFM steel was irradiated with 100 keV hydrogen ions at 450℃, some dislocations were observed, and a lot of dot precipitates with enriched Cr were produced [9]. In RAFM steel, Nb and Mo which can cause long-term activation under neutron irradiation are replaced by W, V and Ta compared to common martensitic steels. The roles of these micro-alloying elements (V, Ti, and W) in RAFM steel are very important. Generally, V as effective strengthener is added into steel because V based carbides with small size play a crucial role in pinning grain boundaries, and improving strength and work hardening [10]. However, the irradiation effects of V in RAFM steel is not very clear from the previous reports. In order to clarify the irradiation effects and metallurgic performance of V in RAFM steel, Fe-0.2wt.%V model alloy was designed, and the effect of V will be easy to be identified via comparing the Fe-0.2wt%V alloy and pure Fe. In this work, the effects of hydrogen-ion irradiation on microstructure and hardness were investigated in detail.

Zhang, Yongqin Chang, Yongwei Wang, Xiaolin Li, Shaoning Jiang, Farong Wan, and Yi Long are with the School of Materials Science and Engineering, University of Science and Technology Beijing, Beijing 100083, China (corresponding author phone: 86-10-62334958; e-mail: chang@ustb.edu.cn).

II. Experiments

Fe-0.2wt.%V alloy and pure Fe (99.999%) were chosen for irradiation experiments. Fe-0.2wt.%V alloy was prepared by vacuum arc melting furnace with pure Fe (99.999%) and V (99.9%) as source materials. The content of V is the same as it in RAFM steel (Cr 9.0, C 0.10, Mn 0.45, W 1.50, Ta 0.07, V 0.20, and Fe balanced). The specimens suitable for TEM studies were first ground to about 0.1 mm in thickness and punched out to disks with the diameter of 3 mm, afterward, they were polished using a twin-jet electro-polisher with a polishing solution of $5HCLO_4$+95%C_2H_5OH compound. In order to understand the irradiation effect of hydrogen ions, the specimens were then irradiated with 100 keV H ions by a BNU-400 ion accelerator at room temperature to ion fluences of $1\times10^{17}cm^{-2}$. The detailed irradiation conditions were summarized in Table I. Pure Fe was also irradiated at the same condition for comparison. The irradiated samples were then followed by annealing at 773 K for 1.5 h to evaluate the development of the irradiation defects.

TABLE I
H-Ion Irradiation Conditions for Fe-0.2wt.%V Alloy and Pure Fe

Ions	Energy (keV)	Fluence (ions/cm^2)	Current (μA)	Time (min.)	Temperature
H	100	1×10^{17}	100	50	Room temperature

Displacements per atom (dpa) and implanted ion profiles were simulated using the stopping and range of ions in matter (SRIM) code for Fe-0.2wt.%V alloy. The microstructures of the samples were analyzed using a SUPRA 55 scanning

electron microscope (SEM) and JEM-2010 analytical transmission electron microscope (TEM). Selected area electron diffraction (SAED) analysis and energy dispersive X-ray spectroscopy (EDS) were carried out for precipitates identification. Microhardness was measured both prior to and after irradiation by hydrogen ions. Nano-indentation tests were performed on MTS Inc. (USA) Nano Indenter II at room temperature. The direction of the indentation was chosen to be parallel to ion-beam axis, or normal to the irradiated surface. The indenter tip was Berkovich triangular pyramid.

III. Results and Discussion

The damage profiles of irradiation dose and H ions distribution for Fe-0.2wt.%V alloy were determined using SRIM 2008.01 full-cascade simulations under the assumptions of density of 7.86 g/cm^3 and threshold displacement energies of 40 eV [11]. The distribution of radiation damage and H ion concentration as function of depth in specimen were shown in Fig. 1. The predicted maximum dose is of around 0.45 dpa, and the peak position of H ions concentration locates at 483 nm.

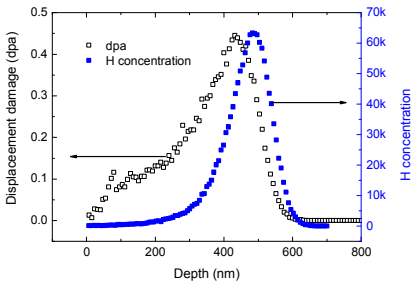

Fig. 1 SRIM predications for 100 keV H-ion irradiation in Fe-0.2wt.%V alloy to ion fluence of 1×10^{17}cm^{-2}

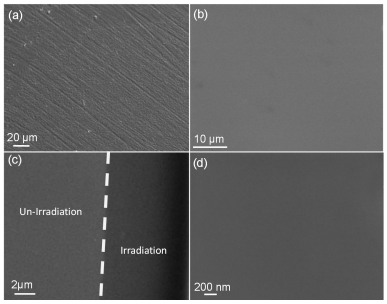

Fig. 2 Surface morphology for Fe-0.2wt.%V alloy. (a) un-electro-polished surface and (b) electro-polished surface of the specimen; (c) with and without irradiation region of the specimen; (d) enlarged part of the irradiation region.

The representative SEM image of Fe-0.2wt.%V alloy with and without H-ion irradiation were shown in Fig. 2. Prior to irradiation, the specimen was mechanically polished to a fine grit of #2000, and the surface morphology was shown in Fig. 2 (a), many scratches are distributed randomly on the surface of the specimen. As the surface was electro-polished at -40℃, it turns to be much clean and flat (Fig. 2 (b)). When the specimen was irradiated by H ions, the entire irradiated surface seems to keep flat with a little deep color compared with the un-irradiated area (Fig. 2 (c)). Fig. 2 (d) is the enlarged part of Fig. 2 (c), which confines that the irradiated surface is quite clean instead of sputtering erosion. There is no obvious difference between the un-irradiated region and irradiated region, which might relate to the low irradiation dose in this work.

The general views of the un-irradiated microstructure and the detailed arrangement of dislocations in the irradiated specimen were shown in Fig. 3. In the un-irradiated specimen, no dislocation loops are observed (Fig. 3 (a)), while a large amount of defects and defect clusters appear in the H-ion irradiated specimen, and these defects are not uniform in size and some of them are tangled (Fig. 3 (b)). Fig. 3 (c) is the dark-field TEM image for Fe-0.2wt.%V alloy taken on the same region of Fig. 3 (b), which indicates that these defects are dislocations. The right-up inset of Fig. 3 (b) is the corresponding SAED pattern, which shows that there are no extra diffraction spots except of the matrix. It also confines that the tiny blank spots are not precipitates but irradiation defects induced by H-ion irradiation. Slight defocused bright-field TEM images were taken to enhance the contrast of the dislocation loops, and the results were shown in Figs. 3 (d) and 3 (e), it clearly shows that most of defects induced by H-ion irradiation at room temperature are dislocation loops. For comparison, the radiation-induced defects in pure Fe irradiated at the same conditions were shown in Figs. 3 (f) and (g), dislocation loops are also obviously resolved in the irradiated sample, while no obvious defects were detected prior to irradiation for pure Fe (the TEM results were not shown here). Figs. 3 (h) and (i) show the size distribution of the irradiation-induced dislocation loops in Fe-0.2wt.%V alloy and pure Fe, respectively. It reveals that the size of the dislocation loops in Fe-0.2wt.%V alloy is more uniform than that in pure Fe. The average size and density of the dislocation loops in pure Fe and Fe-0.2wt.%V alloy were presented in Table II. The average sizes of the dislocation loops is around 32.0 nm and 21.2 nm for pure Fe and Fe-0.2wt.%V alloy, respectively. The density of the dislocation loops in pure Fe and Fe-0.2wt.%V alloy is 5.4×10^{20}m^{-3} and 9.7×10^{20} m^{-3} respectively. Fig. 3 and Table II reveal that the existing of V in Fe-0.2wt.%V alloy reduces the size and increases the density of the dislocation loops compared with pure Fe. No voids were detected in the irradiated Fe-0.2wt.%V alloy and pure Fe, which closely relates to the fast diffusion rate of H behavior in iron steel with a coefficient of 10^{-8} m^{2}s^{-1} even at room temperature and the low irradiation dose in our work. On the other hand, the voids may be too small to be observed by TEM.

In order to better understand H-ion irradiation effects in fusion reactor, the irradiated Fe-0.2wt.%V alloy was annealed at 773 K for 1.5 h, and the typical low-magnification TEM image of the annealed sample was shown in Fig. 4. It clearly shows that many spots distribute in the matrix, and the black spots in the bright-field TEM image (Fig. 4 (a)) turn to white spots in the dark-field TEM image (Fig. 4 (b)), which indicates that these spots are impurities instead of dislocation loops. Fig. 4 (c) is the enlarged part of Fig. 4 (a), from which the black

contrast areas with the diameter of about 3-6 nm were observed. Fig. 4 (d) illustrates a high-resolution TEM (HRTEM) image of the annealed sample to investigate the defects more clearly. It reveals that the crystal lattice of the spots (marked with circle in Fig. 4 (d)) is quite different with that of the matrix. The SAED pattern of the spots was shown in the right-up inset of Fig. 4 (d), in which some extra diffraction spots of secondary phase were observed, while the SAED result of the matrix only shows the Fe diffraction pattern (inset of Fig. 4 (a)). The EDS examination was also performed to confine the impurity phase, and the results show that the signal of C detected from the spots region (Fig. 4 (e)) is much higher than that detected from the region without spots (Fig. 4 (f)). The typical composition of the spots and the matrix were shown in Table III. Combined the SAED pattern and EDS results of the spots, it can be inferred that some impurity phases were precipitated as the irradiated sample was annealed at 773 K, but the composition and crystal structure of these small precipitates could not be determined due to their small sizes compared to the size of the EDS excited volume. The signal of C maybe comes from the irradiation process, low purity of V source materials or the errors due to environmental contamination during long-time examination. If the effect of the long-time examination was abstracted, the small precipitates still exhibit higher signal of C than that of the matrix. The purity of V used in this work is not very high, some of precipitates with the enriched C maybe origin from the impurity of V, while the total concentration of V in Fe-0.2wt.%V alloy is quite low, so the most of C in the small precipitates may origin from the irradiation process. Some distortions were also observed in Fig. 4 (d). The SAED pattern and the EDS results of the distortions show no obvious difference compared with these of the matrix, which indicates that the distortions are the strain field that gives the contrast. In some region of the annealed sample, some large precipitated phases with the diameter from 47 nm to 113 nm were detected, as shown in Fig. 5. Figs. 5 (a) and (b) are the bright-field and dark-field TEM image, respectively. The EDS result of these precipitates show the typical composition of approximately (in wt.%) 6.2V and 92.2Fe (Fig. 5 (c)), which shows the signal of V is much higher than that of the matrix (Table III).

TABLE II
THE AVERAGE SIZE AND DENSITY OF THE DISLOCATION LOOPS IN THE SPECIMENS EVALUATED FROM TEM IMAGES

Specimen	Mean size (nm)	Density (m^{-3})	Counted defects
Fe	32.0	5.4×10^{20}	80
Fe-0.2wt.%V	21.2	9.7×10^{20}	80

TABLE III
TYPICAL COMPOSITION OF THE SMALL PRECIPITATES, THE LARGE PRECIPITATES AND THE MATRIX (WT.%) IN THE ANNEALED FE-0.2WT.%V ALLOY

	C K	V K	FeK
Small precipitates	10.3	0.4	89.3
Large precipitates	1.6	6.2	92.2
Matrix	3.2	0.5	96.3

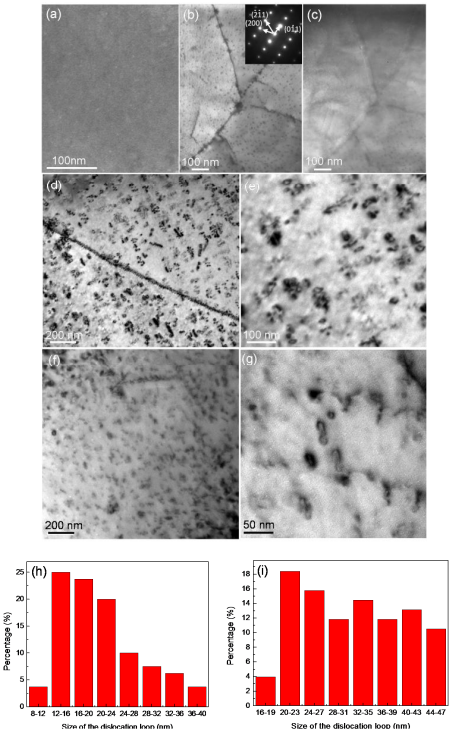

Fig. 3 Low magnification TEM micrographs showing the microstructures of the specimens (a) un-irradiated condition of Fe-0.2wt.%V alloy; (b) bright-filed TEM image (c) dark-field TEM image of the irradiated Fe-0.2wt.%V alloy, the up inset of (b) is the corresponding SAED pattern; (d) dislocation loops in the irradiated Fe-0.2wt.%V alloy; (e) enlarged part of (d); (f) general views of the detailed arrangement of dislocations in the irradiated pure Fe; (g) enlarged part of (f); (h) and (i) showing the size distribution of the dislocation loops in Fe-0.2wt.%V alloy and pure Fe, respectively

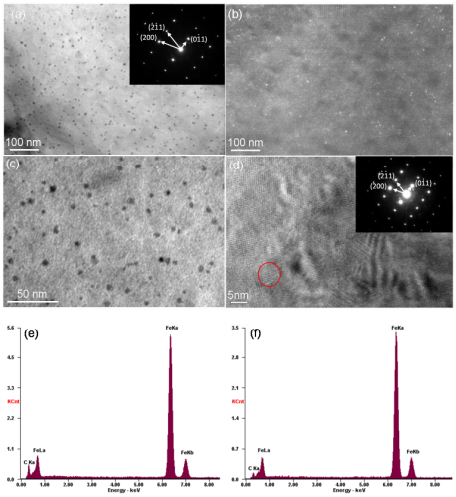

Fig. 4 TEM images of the annealed Fe-0.2wt.%V alloy. (a) bright-filed TEM image, the up-inset is the SAED pattern of the matrix; (b) dark-field TEM image; (c) enlarged part of (a), showing the irradiation-induced small precipitates with the size of 3-6 nm; (d) HRTEM image of the annealed Fe-0.2wt.%V alloy, the right-up inset is the SAED pattern of the spots region; (e) EDS of the region with spots; (f) EDS of the region without spots

Combined the phenomena of the precipitates and the distortions in Figs. 4 and 5, it can be deduced that the atoms of Fe and V are redistributed during the irradiation process, in addition, some C atoms and dislocation loops were also introduced into the materials. When the irradiated specimen was annealed, the diffusion rate of V was accelerated in Fe, and the un-equilibrium atoms cline to group together and form precipitates with enriched V atoms because the solid solubility of V in Fe is very limited according to the Fe-V binary phase diagram. The small precipitates with enriched C atoms have the similar formation process. Some C atoms were introduced into the specimen during the irradiation process, and these C atoms are easy to gather together after annealing treatment. The distortions with the average size of 21 nm in the annealed specimen (Fig. 4 (d)) is comparable to the size of the dislocation loops in the un-annealed specimen (Fig. 3 (e)), from which it can be deduced that the strain flied of the dislocation loops introduced by H-ion irradiation maybe releases in some degree as the specimen was annealed. The dislocation loops disappear, while the residue strain field forms the distortions in the annealed sample, as shown in Fig. 4 (d).

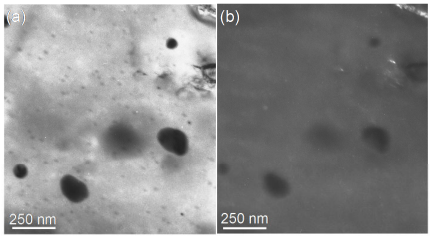

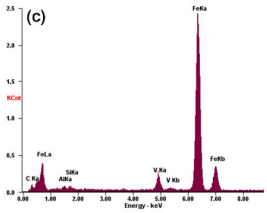

Fig. 5 The bright-field TEM image (a); the dark-field TEM image (b) and the EDS pattern (c) of the large precipitate phases in the annealed Fe-0.2wt. %V alloy

TABLE IV
HARDNESS OF THE UN-IRRADIATED AND IRRADIATED SPECIMENS

Specimen	Un-irradiated specimen (GPa)	Irradiated specimen (GPa)	ΔGPa/original hardness (%)
Fe	1.002	1.065	6.3
Fe-0.2wt.%V	1.158	1.203	3.9

Microhardness was used to estimate changes in mechanical properties during irradiation, and the measurement results for Fe-0.2wt.%V alloy was presented in Table IV along with pure Fe for comparison. The hardness increases after irradiation for both pure Fe and Fe-0.2wt.%V alloy. The irradiation induced hardening is mainly ascribed to the formation of the dislocation loops. Additionally, some precipitations or nano-defects, which are extremely difficult to observe in TEM may also contribute to the hardening in the irradiated specimens. Table IV also shows that the change of irradiation-induced hardness in Fe-0.2wt.%V alloy is smaller than that in pure Fe.

IV. CONCLUSION

This work provides information on the microstructural and hardening changes in Fe-0.2wt.%V alloy and pure Fe irradiated with 100 keV hydrogen ions at room temperature. It was found that the irradiated specimens show no obvious change of the surface because of the low-dose irradiation, while the implanted hydrogen ions have significant effects on microstructural damage, and dislocation loops with small size and high density were introduced. As the irradiated Fe-0.2wt.%V alloy sample was annealed at 773 K, the irradiation-induced dislocation loops disappear, while some distortions form and many small precipitates with enriched C distribute in the matrix. Some large precipitates with a typical composition of approximately (in wt.%) 6.2V and 92.2Fe were also observed. The hardness of the Fe-0.2wt.%V alloy and pure Fe increases after irradiation, which mainly ascribes to the formation of the dislocation loops in the irradiated specimens. Compared with pure Fe, the size of the irradiation-introduced dislocation loops in Fe-0.2wt.%V alloy decreases and the density increases, the change of the hardness also decreases..

ACKNOWLEDGMENT

This project was financially supported by the national natural science foundation of China (no. 11175014, 50971030), national basic research program of china (2009gb109004) and national magnetic confinement fusion program (2011gb108002).

REFERENCES

[1] C. Dethloff, E. Gaganidze, V.V. Svetukhin, J. Aktaa, "Modeling of helium bubble nucleation and growth in neutron irradiated boron doped RAFM steels," *J. Nucl. Mater*., vol. 426, pp. 287-297, July 2012.
[2] W.B. Liu, C. Zhang, Z.G. Yang, Z.X. Xia, G.H. Gao, Y.Q. Weng, "Effect of surface nanocrystallization on microstructure and thermal stability of reduced activation steel," *Acta Metallurgica Sinica,* vol. 49, pp. 707-716, Jun. 2013.
[3] Z. Jiao, N. Ham, G.S. Was, "Microstructure of helium-implanted and proton-irradiated T91 ferritic/martensitic steel," *J. Nucl. Mater*. vol. 367, pp. 440-445, Aug. 2007.
[4] I.I. Chernov, S.Y. Binyukov, B.A. Kalin, M. Win,T.Swe, S.V. Chubarov, A.N. Kalashnikov, A.G. Ioltukhovskiy, M.V. Leontyeva-Smirnova, "Behavior of helium in steel 16Cr12W2VTaB under various implantation temperatures," *J. Nucl. Mater.,* vol. 367, pp. 468-472, Aug. 2007.
[5] H. Ogiwara, A. Kohyama, H. Tanigawa, H. Sakasegawa, "Helium effects on mechanical properties and microstructure of high fluence ion-irradiated RAFM steel," *J. Nucl. Mater.,* vol. 367, pp. 428-433, Aug. 2007.
[6] C. Liu, H. Klein, P. Jung, "Embrittlement of RAFM EUROFER97 by implanted hydrogen," *J. Nucl. Mater*., vol. 335, pp. 77-82, Oct. 2004.
[7] T. Hino, Y. Katada, Y. Yamauchi, M. Akiba, S. Suzuki, T. Ezato, "Deuterium retention of ferritic steel irradiated by energetic hydrogen ions," *J. Nucl. Mater.,* vol. 386-388, pp. 736-739, Apr. 2009.
[8] Y.N. Huang, F.R. Wan, X. Xiao, S. Shi, Y. Long, S. Ohnuki, N. Hashimoto, "The effect of isotope on the interaction between hydrogen and irradiation defect in pure iron," *Fusion Eng. Des.,* Vol. 85, pp. 2203-2206, Sept. 2010.

[9] F. Zhao, F.R. Wan, "Microstructure change of reduced activation Ferritic/Martensitic steels after ion irradiation," *J. Nanjing University,* vol. 45, pp. 258-263, Apr. 2009.
[10] M. PapaRao, V.S. Sarma, S. Sankaran, "Development of high strength and ductile ultra-fine grained dual phase steel with nano sized carbide precipitates in a V-Nb microalloyed steel," *Mater. Sci. Eng. A,* vol. 568, pp. 171-175, Jan. 2013.
[11] M. Ando, H. Tanigawa, S. Jitsukawa, T. Sawai, Y. Katoh, A. Kohyama, K. Nakamura, H. Takeuchi, "Evaluation of hardening behaviour of ion irradiated reduced activation ferritic/martensitic steels by an ultra-micro-indentation technique," *J. Nucl. Mater*., Vol. 307-311, pp. 260-265, Dec. 2002.

Yongqin Chang graduated from State Key Laboratory of Solidification Processing, Northwestern Polytechnical University, Xi'an, China, For BE, ME and PhD Degrees from 1996 to 2002 (with Prof. Jie Wanqi). She worked in National Lab of Mesoscopic Physics & Electron Microscopy Lab, Peking University, as Postdoc (with Prof. D. P. Yu) from 2002 to 2004. She works for School of Materials Science and Engineering, University of Science and Technology Beijing since 2004. She worked in Oak Ridge National laboratory (USA) as a visiting scientist from 2010 to 2011.

She works in irradiation materials science field. She is supported by more than ten findings, such as National Natural Science Foundation of China, Beijing Natural Science Foundation, National Basic Research Program of China and 973. Now she has published more than 70 papers (some papers have been cited more than 400 times).

Prof. Chang was awarded New Century Excellent Talents in University (2007) and Beijing Novel Program (2006) for her outstanding research contribution.